



ELSEVIER

Journal of Alloys and Compounds 266 (1998) 54–60

Journal of  
ALLOYS  
AND COMPOUNDS

# Antiferromagnetic order in the $\text{ThCr}_2\text{Si}_2$ type phosphides $\text{CaCo}_2\text{P}_2$ and $\text{CeCo}_2\text{P}_2$

M. Reehuis<sup>a,b</sup>, W. Jeitschko<sup>a,\*</sup>, G. Kotzyba<sup>a</sup>, B. Zimmer<sup>a</sup>, X. Hu<sup>b</sup>

<sup>a</sup>Anorganisch-Chemisches Institut, Universität Münster, Wilhelm-Klemm-Strasse 8, D-48149 Münster, Germany

<sup>b</sup>Hahn-Meitner-Institut, Glienicker Strasse 100, D-14109 Berlin, Germany

Received 19 August 1997

## Abstract

Magnetic susceptibility and neutron powder diffraction experiments reveal that the cobalt atoms in  $\text{CaCo}_2\text{P}_2$  and  $\text{CeCo}_2\text{P}_2$  order antiferromagnetically below the Néel temperatures  $T_N=113(2)$  K and  $T_N=440(5)$  K, respectively. In these tetragonal compounds with  $\text{ThCr}_2\text{Si}_2$  type structure ( $I4/mmm$ ) the magnetic moments of the cobalt atoms are ordered ferromagnetically within the basal plane and antiferromagnetically along the  $c$  axis with the stacking sequence  $+-, +-$ , corresponding to a propagation vector  $\mathbf{k}=(0, 0, 1)$ . In the calcium compound the cobalt moments with  $\mu_{\text{exp}}=0.32(2)$   $\mu_{\text{B}}$  are ordered perpendicular to the  $c$  axis, whereas in the cerium compound these moments with  $\mu_{\text{exp}}=0.94(2)$   $\mu_{\text{B}}$  are aligned parallel to this axis. The magnetic properties of the previously investigated cobalt containing phosphides  $\text{ACo}_2\text{P}_2$  ( $\text{A}=\text{Sr}, \text{La}, \text{Pr}, \text{Nd}, \text{Sm}, \text{Eu}$ ) are briefly reviewed. The magnetic ordering temperatures and the magnetic moments of the cobalt atoms correlate with the formal charge of the cobalt-phosphorus polyanion and with the Co–Co distances.

© 1998 Elsevier Science S.A.

**Keywords:** Ternary cobalt phosphides; Magnetic susceptibility; Neutron diffraction; Magnetic structure

## 1. Introduction

The magnetic properties of the  $\text{ThCr}_2\text{Si}_2$  type lanthanoid (Ln) transition metal (T) silicides  $\text{LnT}_2\text{Si}_2$  and germanides  $\text{LnT}_2\text{Ge}_2$  have been reported by several groups [1–10]. The corresponding phosphides  $\text{LnT}_2\text{P}_2$  are also known for some time [11–13] and their magnetic properties have been investigated. The nickel and iron atoms of the series  $\text{LnFe}_2\text{P}_2$  [14,15] and  $\text{LnNi}_2\text{P}_2$  [16] do not carry magnetic moments. Of the cobalt compounds  $\text{SrCo}_2\text{P}_2$  shows enhanced Pauli paramagnetism [14,15]. A single-crystal neutron diffraction investigation of  $\text{EuCo}_2\text{P}_2$  revealed magnetic moments only for the europium positions [17], whereas magnetic order of the cobalt moments was reported for  $\text{LaCo}_2\text{P}_2$  [14,15,18],  $\text{PrCo}_2\text{P}_2$  and  $\text{NdCo}_2\text{P}_2$  [15,19]. In the present paper we give an account of the magnetic properties of  $\text{CaCo}_2\text{P}_2$  and  $\text{CeCo}_2\text{P}_2$ . We also

briefly review the magnetic properties of all isotypic cobalt containing  $\text{ThCr}_2\text{Si}_2$  type phosphides.

## 2. Experimental

The samples of  $\text{CaCo}_2\text{P}_2$  and  $\text{CeCo}_2\text{P}_2$  were prepared from a tin flux as described earlier [13]. Starting materials (with nominal purities all >99.9%) were filings of calcium or cerium and powders of cobalt and tin. The red phosphorus was in the form of small pieces (Hoechst, Knap-sack: ultrapure). The filings of calcium and cerium were stored under oil, which was washed away with dried n-hexane before use. The mixtures with the atomic ratio  $\text{Ca}(\text{Ce}): \text{Co}: \text{P}: \text{Sn}=1:2:2:20$  were annealed in evacuated, sealed silica tubes for 8 days at 950°C and subsequently quenched in water. The tin-rich matrix was dissolved in slightly diluted (1:1) hydrochloric acid. The products were identified by their Guinier powder diagrams.

Susceptibility measurements were carried out with a SQUID magnetometer in the temperature range between 2

\*Corresponding author. Tel.: +49 251 833 3121; fax: +49 251 833 3136.

K and 350 K using magnetic flux densities of up to 5.5 T and with sample masses up to 20 mg. In the case of  $\text{CaCo}_2\text{P}_2$  two oriented single crystals (2.54 mg) were glued on a thin glass fibre and were placed in the SQUID magnetometer with the tetragonal  $c$  axis parallel and subsequently also perpendicular to the applied magnetic field.

The neutron powder diffraction measurements were carried out on the E6 instrument at the reactor BER II of the Hahn-Meitner-Institut in Berlin. This instrument has a double focussing graphite monochromator using the reflection 002 ( $\lambda=238$  pm). Three data sets at different temperatures were collected for both compounds in the  $2\theta$  range between 10–90° with a 20° multidetector. For the cerium compound further 16 data sets were measured in the range 10–70° at different temperatures between 2 K and 474 K. Further details of the E6 instrument are described elsewhere [20].

The Rietveld refinements of the neutron powder diffraction data were carried out with the program FULLPROF [21]. The nuclear scattering lengths used were  $b(\text{Ca})=4.90$  fm,  $b(\text{Ce})=4.82$  fm,  $b(\text{Co})=2.50$  fm and  $b(\text{P})=5.13$  fm [22]. The magnetic form factor for the cobalt atoms was taken from Ref. [23] assuming  $\text{Co}^{1+}$ , however, the results do not change much when the form factors of  $\text{Co}^0$  or  $\text{Co}^{2+}$  are used.

### 3. Results and discussion

#### 3.1. SQUID magnetometry

The results of our magnetic susceptibility measurements for powder and single crystals of  $\text{CaCo}_2\text{P}_2$  are shown in Fig. 1. Essentially they agree with our earlier measurements of a powder sample recorded with a Faraday balance [15]. The powder data show a broad minimum at about 20 K and a discontinuity above 100 K. The minimum at 20 K is more pronounced in the reciprocal susceptibility curve recorded from single-crystals with the external field parallel to the  $c$  axis. The neutron diffraction results did not suggest any phase transition to be associated with this minimum. The minimum has already been observed earlier [15], where it was ascribed to an exchange enhanced Pauli paramagnetism. The discontinuity of the powder data at higher temperature corresponds to a minimum of the single-crystal data obtained with the magnetic field perpendicular to the  $c$  axis. The neutron diffraction results, discussed below, revealed this minimum at  $113\pm 2$  K to be due to the ordering temperature of the cobalt moments.

The reciprocal susceptibility of the cerium compound (Fig. 1, bottom) is reproduced here [15] for completeness. The minimum at  $440\pm 5$  K corresponds to the Néel temperature. The neutron diffraction data did not indicate a further magnetic phase transition at lower temperature,

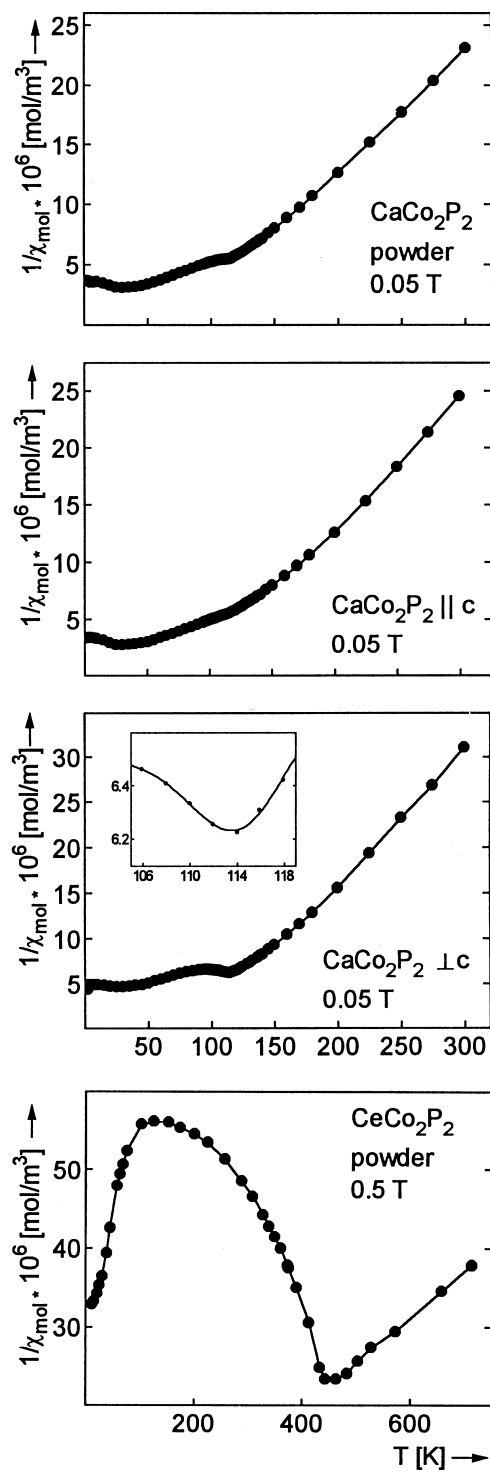


Fig. 1. Temperature dependence of the reciprocal magnetic susceptibility of  $\text{CaCo}_2\text{P}_2$  and  $\text{CeCo}_2\text{P}_2$ . The results obtained for the powder sample of  $\text{CaCo}_2\text{P}_2$  are compared to those for single crystals with the external magnetic field of 0.05 T aligned parallel and perpendicular to the  $c$  axis of the tetragonal crystals. The powder data for the cerium compound were taken from [15].

hence the downturn of the reciprocal susceptibility below 200 K may possibly be due to an impurity.

Magnetization isotherms were recorded for both  $\text{CaCo}_2\text{P}_2$  and  $\text{CeCo}_2\text{P}_2$  up to magnetic flux densities of 5.5 T. These showed the linear dependencies as is usually found for regular antiferromagnets. No indications for metamagnetism were observed.

### 3.2. The nuclear structures

The  $\text{ThCr}_2\text{Si}_2$  type structure (Fig. 2) of  $\text{CaCo}_2\text{P}_2$  and  $\text{CeCo}_2\text{P}_2$  was confirmed and refined from the neutron powder diffraction data (Fig. 3) recorded at various temperatures. A total of 10 variable parameters was refined: an overall scale factor, five peak shape parameters, the zero point, two lattice constants and the positional parameter  $z$  of the phosphorus atom. One isotropic displacement parameter  $B=0.3 \times 10^4 \text{ pm}^2$  for the three atomic sites was held constant. When occupancy parameters were refined no significant deviations from the ideal values were observed, thus the ideal values were assumed during the

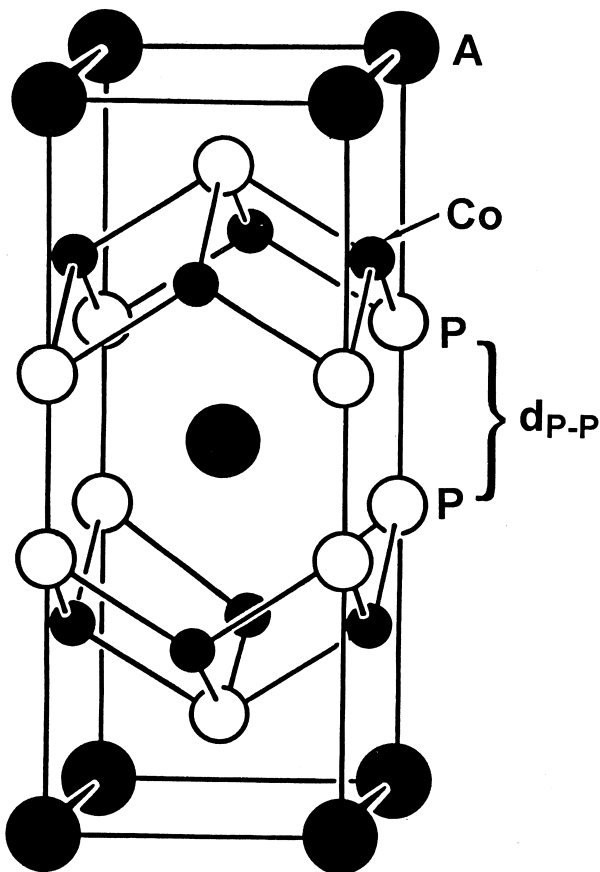


Fig. 2. The tetragonal ( $I4/mmm$ )  $\text{ThCr}_2\text{Si}_2$  type structure of the phosphides  $\text{ACo}_2\text{P}_2$ , where A is an alkaline, alkaline earth or a rare earth metal. Two branches of this structure may be distinguished: one with P–P-bonds ( $220 \text{ pm} < d_{\text{P-P}} < 270 \text{ pm}$ ) and one, where the P–P distances are greater ( $> 280 \text{ pm}$ ), and phosphorus–phosphorus bonding can be excluded.

last refinement cycles. The results are summarized in Table 1. The positional parameters  $z=0.3742(8)$  and  $z=0.3714(7)$  obtained at 270 and 300 K for the calcium and the cerium compounds, respectively, are in good agreement with the previously reported values  $z=0.3721(4)$  [28] and  $z=0.3718(3)$  [13].

The cell volumes of the series  $\text{LnCo}_2\text{P}_2$  show a relatively large anomaly for the cerium compound, and it has been suggested, that cerium might be tetravalent or it might have a mixed or intermediate valence in  $\text{CeCo}_2\text{P}_2$  [13]. We therefore investigated the temperature dependence of the lattice constants of this phosphide. For this purpose we collected neutron powder diffraction data of  $\text{CeCo}_2\text{P}_2$  up to  $2\theta=70^\circ$  at temperatures between 2 and 440 K. The cell volumes and the  $c/a$  ratios resulting from the evaluation of these data are plotted in Fig. 4 together with a few corresponding values for  $\text{CaCo}_2\text{P}_2$  (Table 1),  $\text{PrCo}_2\text{P}_2$  (at 503 K:  $a=389.9(1) \text{ pm}$ ,  $c=987.6(3) \text{ pm}$ ) and  $\text{NdCo}_2\text{P}_2$  (at 503 K:  $a=389.1(1) \text{ pm}$ ,  $c=973.8(3) \text{ pm}$ ) determined during the present investigation and in part also previously [19]. It can be seen that the cell volume of the cerium compound shows a more pronounced increase with temperature than the volumes of the other phosphides with this structure. This suggests that the cerium atoms become increasingly trivalent at higher temperature. On the other hand, at lower temperatures (up to about 300 K) the thermal expansion of  $\text{CeCo}_2\text{P}_2$  does not differ very much from the thermal expansion of the other compounds. Hence, it seems justified to regard the cerium atoms as essentially tetravalent below 300 K, especially also since the cell volume of  $\text{CeCo}_2\text{P}_2$  is considerably smaller than that of  $\text{PrCo}_2\text{P}_2$  [15]. An even more pronounced increase with rising temperature can be seen for the  $c/a$  ratio of  $\text{CeCo}_2\text{P}_2$ . This has to do with the weakening of P–P bonds within the P<sub>2</sub> pairs, as is discussed further below.

### 3.3. The magnetic structures

The neutron powder diffraction data of  $\text{CaCo}_2\text{P}_2$  and  $\text{CeCo}_2\text{P}_2$  recorded at 2 K showed additional peaks (Fig. 3), which can be ascribed to the magnetic order of the cobalt moments. These are listed in Table 2. In general, these magnetic reflections  $(hkl)_M$  can be generated from the nuclear reflections  $(hkl)_N$  of the tetragonal body centered structure by the relation  $(hkl)_M = (hkl)_N \pm \mathbf{k}$ , where  $\mathbf{k}$  is the propagation vector. For both structures this vector was observed to be  $\mathbf{k}=(001)$ . This means that the cobalt moments of both structures are ordered ferromagnetically within the basal *ab* plane and with antiferromagnetic coupling along the *c* axis with the sequence +–, +–. In the case of  $\text{CaCo}_2\text{P}_2$  a reflection  $(001)_M$  was observed, and this indicates that the magnetic moments of the cobalt atoms are oriented perpendicular to the *c* axis (Fig. 5). In contrast, for the cerium compound the reflection  $(111)_M$  is relatively strong. This suggests that the cobalt moments are oriented parallel to the *c* axis.

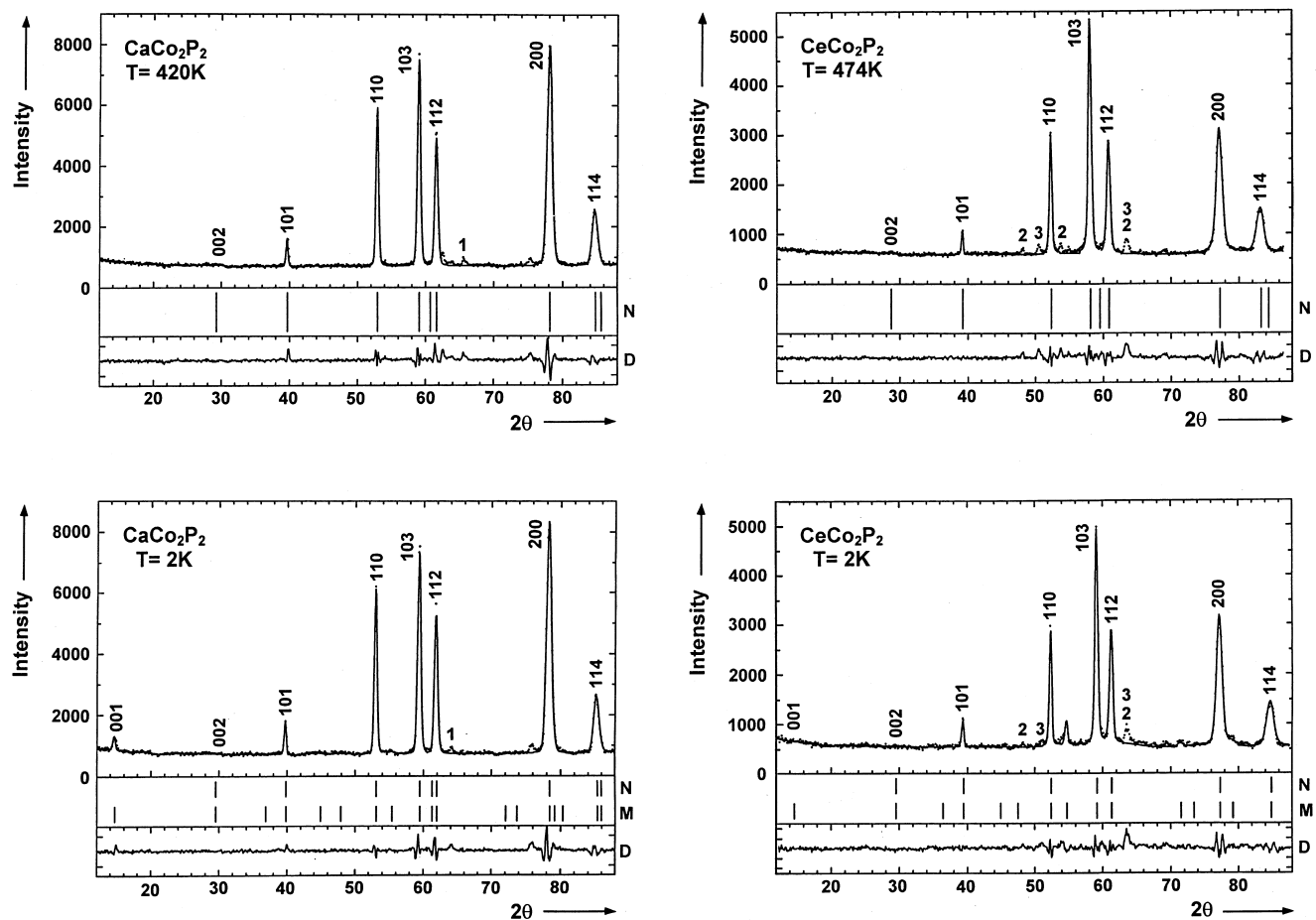


Fig. 3. Neutron diffraction patterns of  $\text{CaCo}_2\text{P}_2$  and  $\text{CeCo}_2\text{P}_2$ . The peak positions of the nuclear (N) and the magnetic (M) structures as well as the differences (D) between the observed and calculated patterns are shown. The samples contained small amounts of impurities; the strongest peaks of each are marked:  $\text{Ca}_2\text{Co}_{12}\text{P}_7$  (1) with the hexagonal  $\text{Zr}_2\text{Fe}_{12}\text{P}_7$  type structure [24],  $\text{Ce}_2\text{Co}_{12}\text{P}_7$  (2) [25,26] and  $\text{CeCoPO}$  (3) [27].

These models for the magnetic structures of  $\text{CaCo}_2\text{P}_2$  and  $\text{CeCo}_2\text{P}_2$  were successfully refined using the data up to  $2\theta=75^\circ$ . During the final refinement cycles only the magnitudes of the magnetic moments of the cobalt atoms were allowed to vary. These results are also summarized in

Table 1. The magnetic structures of  $\text{CaCo}_2\text{P}_2$  and  $\text{CeCo}_2\text{P}_2$  are shown in Fig. 5 together with the magnetic structures of the other cobalt containing phosphides  $\text{LnCo}_2\text{P}_2$ .

The temperature dependence of the magnetic structures of the calcium and the cerium compounds was monitored

Table 1

Rietveld refinement results of the nuclear and magnetic structures of the tetragonal phosphides  $\text{CaCo}_2\text{P}_2$  and  $\text{CeCo}_2\text{P}_2$

	$\text{CaCo}_2\text{P}_2$			$\text{CeCo}_2\text{P}_2$		
	420 K	270 K	2 K	474 K	300 K	2 K
$a$ [pm]	386.21(15)	385.75(13)	385.13(6)	389.19(9)	389.35(11)	388.87(9)
$c$ [pm]	963.6(5)	959.6(4)	955.5(2)	979.1(3)	959.9(3)	953.3(3)
$c/a$	2.495	2.488	2.481	2.516	2.465	2.451
$V$ [nm <sup>3</sup> ]	0.1437(2)	0.1428(2)	0.1417(1)	0.1483(1)	0.1455(1)	0.1442(1)
$z(\text{P})$	0.3722(6)	0.3742(8)	0.3745(7)	0.3696(10)	0.3714(7)	0.3715(6)
$d_{\text{P-P}}$ [pm]	246.3	241.4	239.8	255.3	246.9	245.0
$R_{\text{N}}$	0.023	0.022	0.021	0.017	0.016	0.015
$\mu_{\text{exp}}(\text{Co})$ [ $\mu_{\text{B}}$ ]	0	0	0.32	0	0.85(3)	0.94(3)
$R_{\text{M}}$	—	—	0.089	—	0.11	0.090

The residuals for the nuclear structure  $R_{\text{N}}$  (defined as  $R_{\text{N}} = \sum \|F_{\text{o}} - |F_{\text{c}}|\| / \sum |F_{\text{o}}|$ ) and the magnetic structure  $R_{\text{M}}$  (defined as  $R_{\text{M}} = \sum \|I_{\text{o}} - |I_{\text{c}}|\| / \sum |I_{\text{o}}|$ ) were obtained in refinements of the diffraction data between  $2\theta$  from  $10^\circ$  and  $90^\circ$  and  $10^\circ$  to  $75^\circ$ , respectively. The isotropic thermal parameter  $B = 0.3 \times 10^4 \text{ pm}^2$  was used for all atoms and was held constant during the refinements.

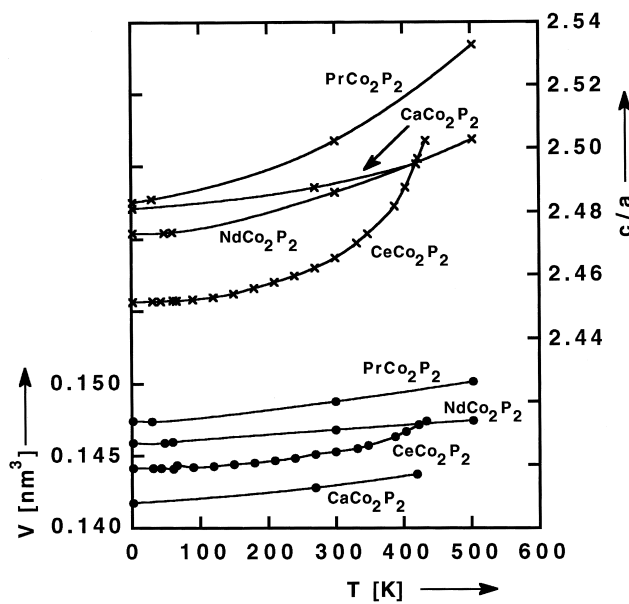


Fig. 4. Thermal variation of the ratios  $c/a$  and the cell volumes of the tetragonal phosphides  $ACo_2P_2$  ( $A=Ca, Ce, Pr, Nd$ ).

Table 2  
Observed and calculated intensities of the magnetic reflections  $(hkl)_M$  of  $CaCo_2P_2$  and  $CeCo_2P_2$  at 2 K

$(hkl)_M$	$CaCo_2P_2$		$CeCo_2P_2$	
	$I_o$	$I_c$	$I_o$	$I_c$
001	265	257	—	0
100	—	0	—	0
003	21	19	—	0
102	—	0	—	0
111	14	31	278	292
113	16	15	106	78
104	—	0	—	0

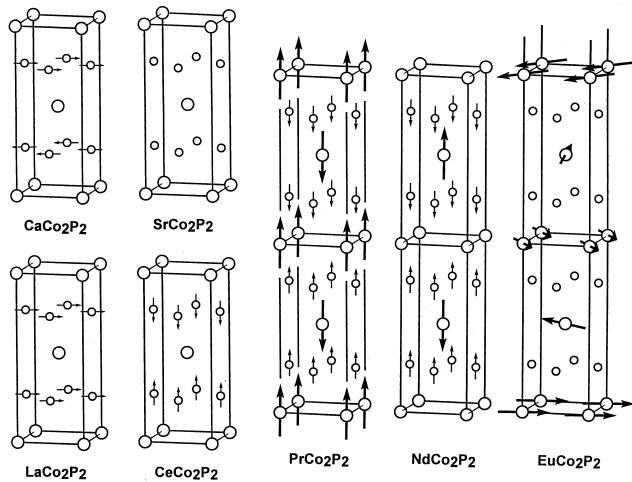


Fig. 5. Magnetic structures of the phosphides  $ACo_2P_2$ , where  $A=Ca, Sr, La, Ce, Pr$  and  $Eu$ . The cobalt atoms (small circles) with their ordered magnetic moments are shown together with the A atoms (large circles), which are in the positions  $(0\ 0\ 0)$  and  $(1/2\ 1/2\ 1/2)$  of the body-centered nuclear cell.

by measuring the intensities of the relatively strong magnetic peaks  $(001)_M$  and  $(111)_M$ , respectively, at various temperatures. In both cases these peaks vanished at the Néel temperatures of  $114 \pm 3$  K and  $440 \pm 5$  K, respectively. This is shown in more detail for  $CaCo_2P_2$  in Fig. 6.

### 3.4. Correlations between structural and magnetic properties

Various aspects of chemical bonding in the phosphides with  $ThCr_2Si_2$  type structure have been discussed using simple bonding models like the Zintl-Klemm concept [11–16], extended Hückel [29] and first principles calculations [30]. The correlation between the  $c/a$  ratios and the P–P distances is known for some time [13]. In Fig. 7 we have plotted these variables as a function of the ionic radii of

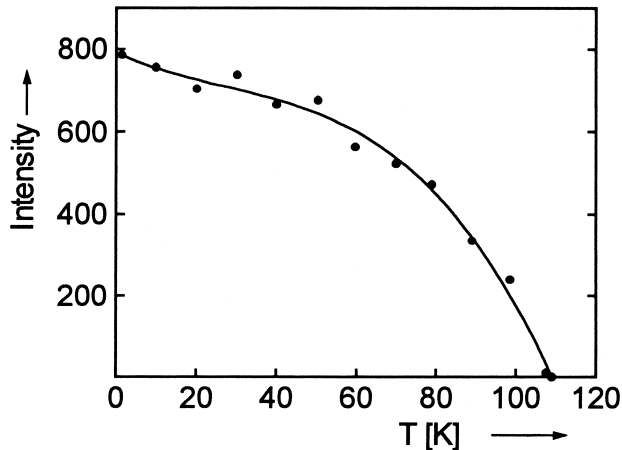


Fig. 6. Temperature dependence of the intensity of the magnetic reflection  $(001)_M$  for the phosphide  $CaCo_2P_2$ . The continuous line is only a guide for the eye.

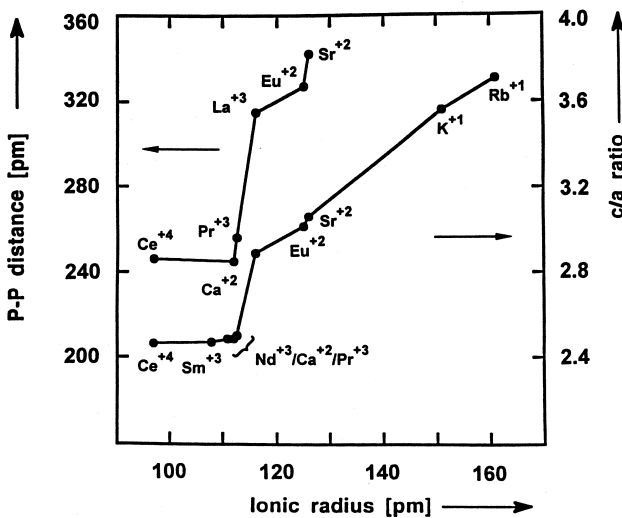


Fig. 7. Correlations between the  $c/a$  ratios, the P–P distances and the ionic radii of the  $A^{+}$  ions in the ternary phosphides  $ACo_2P_2$ . The values of the structural parameters were taken from references 13 and 28.

the A component (taken from reference [31] with the coordination number CN=VIII) of the cobalt containing series  $ACo_2P_2$  (A=K, Rb, Ca, Sr, La, Ce, Pr, Nd, Sm, Eu). It can be seen that the  $c/a$  ratios as well as the P–P distances correlate with the ionic radii. A discontinuity occurs in these curves for a radius of about 115 pm. This suggests potential displacive phase transitions which already have been predicted from theoretical considerations [29] and found for the solid solutions  $Ca_{0.6}Sr_{0.4}Co_2P_2$  [32],  $SrNi_2P_{2-x}As_x$ ,  $Sr_{1-x}Eu_xNi_2P_2$ ,  $SrNi_{2-x}Cu_xP_2$  [33] and  $EuRh_2P_{2-x}As_x$  [34] as a function of composition or temperature, and for the compounds  $SrRh_2P_2$  and  $EuRh_2P_2$  as a function of pressure [35].

The cobalt atoms in the compounds  $ACo_2P_2$  with  $ThCr_2Si_2$  type structure (Fig. 2) form a square grid, which extends parallel to the  $ab$  plane. Hence, the Co–Co distances are a function of the length of the  $a$  axis and this length in turn is also a function of the  $c/a$  ratio. In Fig. 8a,

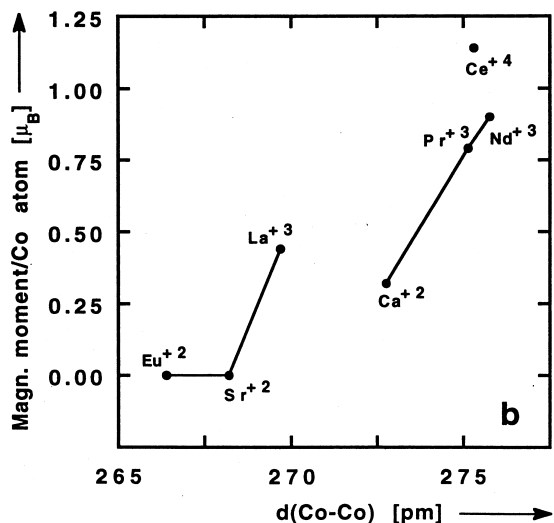
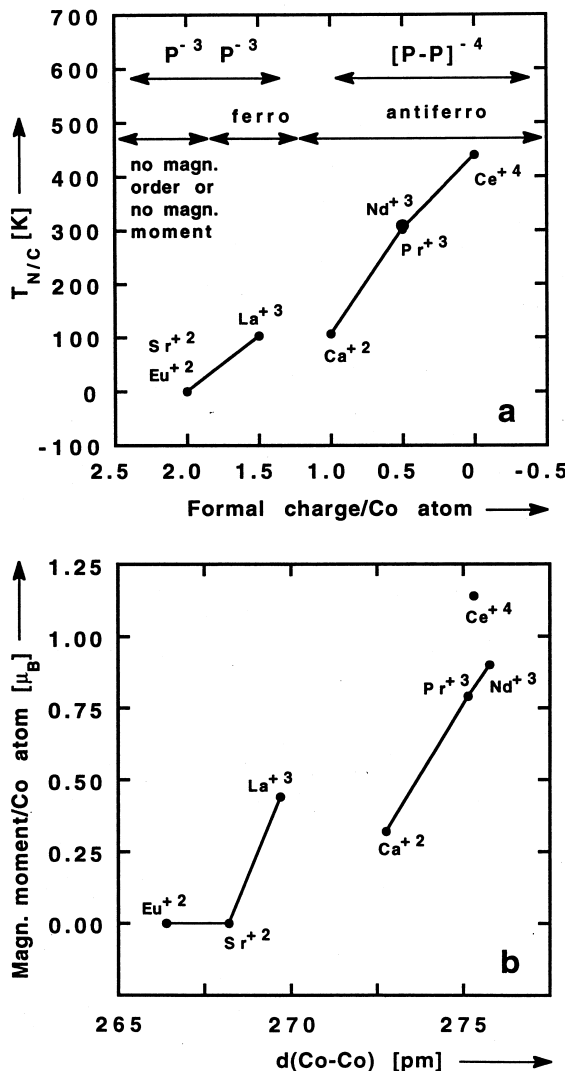


Fig. 8b and Fig. 8c we have plotted the ordering temperatures  $T_C$  and  $T_N$  of the cobalt containing  $ThCr_2Si_2$  type phosphides as well as the magnetic moments per cobalt atom of these compounds as functions of the Co–Co distances and the formal charge per cobalt atom.<sup>1</sup> The region of the potential phase transitions mentioned above is visible in these diagrams between the compounds  $CaCo_2P_2$  and  $LaCo_2P_2$  (labeled  $Ca^{+2}$  and  $La^{+3}$ , respectively).

It can be seen from Fig. 8 that the formal charge/Co atom correlates with the type of magnetism. For a value of 2.0 for this formal charge ( $SrCo_2P_2$  and  $EuCo_2P_2$ ) no

<sup>1</sup>The formal charge (oxidation number) of the cobalt atoms simply follows from the oxidation number of the A atoms and from the oxidation numbers of the ‘isolated’ P atoms (no P–P bonds,  $P^{-3}$ ) or  $P_2$  pairs ( $[P-P]^{-4}$ ), respectively, since the charges have to be balanced in the neutral formula, e.g.  $Ca^{+2}(Co^{+1})_2[P-P]^{-4}$  and  $La^{+3}(Co^{+1.5})_2(P^{-3})_2$ .

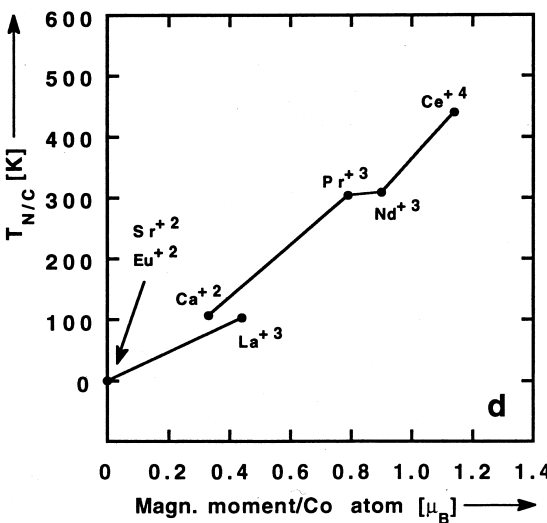
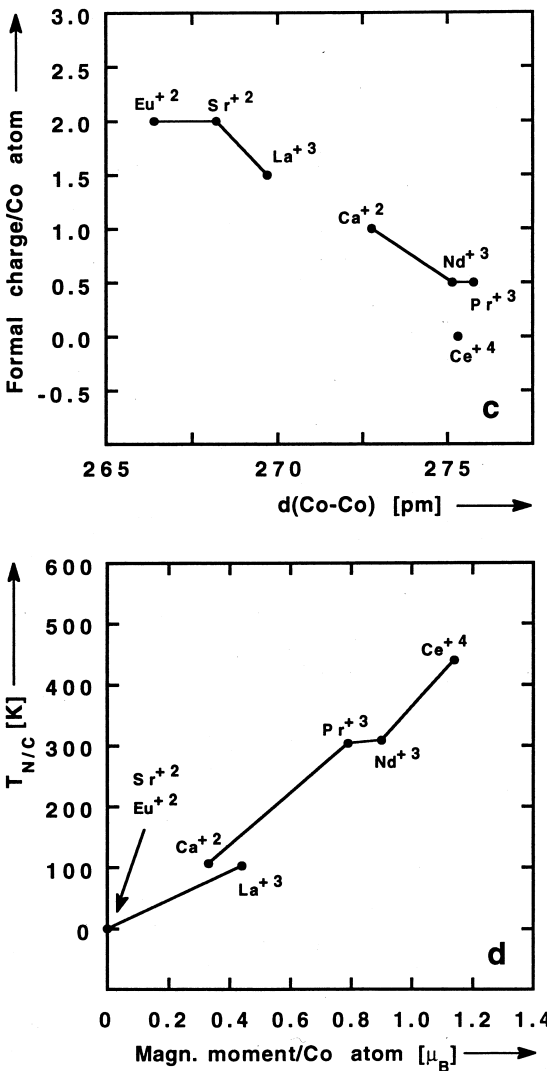


Fig. 8. Correlations between the ordering temperatures and the formal charge per cobalt atom (a), between the magnetic moments and the shortest Co–Co distances (b), between formal charges/Co atom and the shortest Co–Co distances (c) as well as the resulting correlation between the ordering temperatures and the magnetic moment/Co atom (d) in ternary compounds  $ACo_2P_2$  with  $ThCr_2Si_2$  type structure.

magnetic order (or no magnetic moment on the Co atoms) was observed; in  $\text{LaCo}_2\text{P}_2$ , where the Co atoms have a formal charge of 1.5 ferromagnetic order occurs; and in the compounds  $\text{CaCo}_2\text{P}_2$ ,  $\text{PrCo}_2\text{P}_2$ ,  $\text{NdCo}_2\text{P}_2$  and  $\text{CeCo}_2\text{P}_2$  with formal Co charges of 1.0 or less the Co moments order antiferromagnetically. The ordering temperatures  $T_C$  and  $T_N$ , respectively increase with decreasing formal charge. The magnetic moments of these compounds are oriented perpendicular to the  $c$  axes, when the formal charge is high ( $\text{LaCo}_2\text{P}_2$  and  $\text{CaCo}_2\text{P}_2$ ) and they are parallel to this axis when the formal charge is low ( $\text{PrCo}_2\text{P}_2$ ,  $\text{NdCo}_2\text{P}_2$ ,  $\text{CeCo}_2\text{P}_2$ ).

In Fig. 8b we have plotted the values of the magnetic moments per Co atom as a function of the Co–Co distance. From this plot it can be judged that the magnetic moment per cobalt atom increases with the Co–Co distances. This relationship has already been observed for manganese silicides and germanides with  $\text{ThCr}_2\text{Si}_2$  type structure [10].

The plots of Fig. 8a and Fig. 8b look very similar. Since they involve different variables –  $T_{N/C}$  or magnetic moment/Co atom as functions of the formal charge/Co atom or the Co–Co distance – we have also plotted the formal charge/Co atom as a function of the Co–Co distance (Fig. 8c) as well as the ordering temperature  $T_{N/C}$  as a function of the magnetic moment/Co atom (Fig. 8d). Obviously these functions are all interrelated, however, the theoretical interpretation of these interrelationships remains a task for the future.

## Acknowledgements

We are grateful for generous gifts of ultrapure phosphorus (Hoechst AG, Werk Knapsack) and silica tubes (Dr. G. Höfer, Heraeus Quarzschemelze). We also thank Dipl.-Chem. C. Gröver for helpful suggestions and technical support. This work was supported by the Deutsche Forschungsgemeinschaft and the Fonds der Chemischen Industrie.

## References

- [1] I. Mayer, I. Felner, *J. Phys. Chem. Solids* 38 (1977) 1031.
- [2] I. Nowik, I. Felner, M. Seh, *J. Magn. Magn. Mater.* 15–18 (1980) 1215.
- [3] T. Shigeoka, H. Fujii, H. Fujiwara, K. Yagasaki, T. Okamoto, *J. Magn. Magn. Mater.* 31–34 (1983) 209.
- [4] J.W.C. de Vries, R.C. Thiel, K.H.J. Buschow, *J. Less Common Met.* 111 (1985) 313.

- [5] S. Siek, A. Szytuła, J. Leciejewicz, *Solid State Commun.* 39 (1981) 863.
- [6] J. Leciejewicz, A. Szytuła, *Solid State Commun.* 49 (1984) 361.
- [7] P. Schobinger-Papamantellos, Ch. Routsi, J.K. Yakintos, *J. Phys. Chem. Solids* 44 (1983) 875.
- [8] J.M. Barandiaran, D. Gignoux, D. Schmitt, J.C. Gomez Sal, J. Rodriguez-Fernandez, *J. Magn. Magn. Mater.* 69 (1987) 61.
- [9] G. Venturini, R. Welter, E. Ressouche, B. Malaman, *J. Magn. Magn. Mater.* 150 (1995) 197.
- [10] R. Welter, G. Venturini, E. Ressouche, B. Malaman, *J. Alloys Comp.* 218 (1995) 204.
- [11] R. Marchand, W. Jeitschko, *J. Solid State Chem.* 24 (1978) 351.
- [12] W. Jeitschko, B. Jaberg, *J. Solid State Chem.* 35 (1980) 312.
- [13] W. Jeitschko, U. Meisen, M.H. Möller, M. Reehuis, *Z. Anorg. Allg. Chem.* 527 (1985) 73.
- [14] E. Mörsen, B.D. Mosel, W. Müller-Warmuth, M. Reehuis, W. Jeitschko, *J. Phys. Chem. Solids* 49 (1988) 785.
- [15] M. Reehuis, W. Jeitschko, *J. Phys. Chem. Solids* 51 (1990) 961.
- [16] W. Jeitschko, M. Reehuis, *J. Phys. Chem. Solids* 48 (1987) 667.
- [17] M. Reehuis, W. Jeitschko, M.H. Möller, P.J. Brown, *J. Phys. Chem. Solids* 53 (1992) 687.
- [18] M. Reehuis, C. Ritter, R. Ballou, W. Jeitschko, *J. Magn. Magn. Mater.* 138 (1994) 85.
- [19] M. Reehuis, P.J. Brown, W. Jeitschko, M.H. Möller, T. Vomhof, *J. Phys. Chem. Solids* 54 (1993) 469.
- [20] T. Robertson, Neutron scattering. Instrumentation at the Upgraded Research Reactor BER II. Berlin Neutron Scattering Center. BENSC, Berlin, 1992.
- [21] J. Rodriguez-Carvajal, FULLPROF: A Program for Rietveld Refinement and Pattern Matching Analysis, Abstract of the Satellite Meeting on Powder Diffraction of the XV Congress of the IUCr, Toulouse, 1990, p. 127.
- [22] V.F. Sears, Neutron scattering lengths, in: A.J.C. Wilson (Ed.), International Tables of Crystallography, vol. C, Kluwer Academic Press, Dordrecht, 1992, p. 383.
- [23] P.J. Brown, Magnetic form factors, in: A.J.C. Wilson, International Tables of Crystallography, vol. C, Kluwer Academic Press, Dordrecht, 1992, p. 391.
- [24] U. Meisen and W. Jeitschko, unpublished results.
- [25] W. Jeitschko, D.J. Braun, R.H. Ashcroft, R. Marchand, *J. Solid State Chem.* 25 (1978) 309.
- [26] M. Reehuis, W. Jeitschko, *J. Phys. Chem. Solids* 50 (1989) 563.
- [27] B.I. Zimmer, W. Jeitschko, J.H. Albering, R. Glaum, M. Reehuis, *J. Alloys Comp.* 229 (1995) 238.
- [28] A. Mewis, *Z. Naturforsch.* 35b (1980) 141.
- [29] R. Hoffmann, C. Zheng, *J. Phys. Chem.* 89 (1985) 4175.
- [30] E. Gustenau, P. Herzig, A. Neckel, *J. Solid State Chem.* 129 (1997) 147.
- [31] R.D. Shannon, *Acta Crystallogr.* A32 (1976) 751.
- [32] T. Vomhof, Diplomarbeit, Universität Münster, 1989.
- [33] A. Hellmann, V. Keimes, A. Mewis, 7. Vortragstagung der Fachgruppe Festkörperchemie d. GdCh., Bonn, 1994.
- [34] G. Michels, M. Roepke, T. Niemöller, M. Chefki, M.M. Abd-Elmiguid, H. Micklitz et al., *J. Phys. Condens. Matter.* 8 (1996) 4055.
- [35] C. Huhnt, G. Michels, M. Roepke, W. Schlabitz, A. Wurth, A. Mewis, private communication, 1997.